

## Observational evidence of sensitivity of surface climate changes to land types and urbanization

Young-Kwon Lim,<sup>1</sup> Ming Cai,<sup>1</sup> Eugenia Kalnay,<sup>2</sup> and Liming Zhou<sup>3</sup>

Received 1 August 2005; revised 19 September 2005; accepted 19 October 2005; published 30 November 2005.

[1] Sensitivity of surface climate change to land types is investigated for the Northern Hemisphere by subtracting the reanalysis from the observed surface temperature (OMR). The basis of this approach is that while reanalysis represents the large-scale climate changes due to greenhouse gases and atmospheric circulation, it is less sensitive to regional surface processes associated with land types. OMR trends derived from two independent reanalyses (ERA40 and NNR) and two observations (CRU and GHCN) show similar dependence upon land types, suggesting the attribution of OMRs to different land types is robust. OMR trends reveal 1) Warming over barren areas is larger than most other land types. 2) Urban areas show large warming second only to barren areas. 3) Croplands with agricultural activity show a larger warming than natural broadleaf forests. The overall assessment indicates surface warming is larger for areas that are barren, anthropogenically developed, or covered with needle-leaf forests. **Citation:** Lim, Y.-K., M. Cai, E. Kalnay, and L. Zhou (2005), Observational evidence of sensitivity of surface climate changes to land types and urbanization, *Geophys. Res. Lett.*, 32, L22712, doi:10.1029/2005GL024267.

### 1. Introduction

[2] Greenhouse gases [*Intergovernmental Panel on Climate Change*, 2001] and land-uses [*Pielke et al.*, 2002] are known as primary human impacts on climate change. They both contribute to surface warming and reduce the diurnal temperature range [*Gallo and Owen*, 1999; *Kalnay and Cai*, 2003, hereinafter referred to as KC; *Kalnay et al.*, 2005]. It has been suggested that land-use impact on surface climate change is not negligible compared to atmospheric greenhouse effect [*Lofgren*, 1995; *Bounoua et al.*, 1999; KC].

[3] However, an assessment of the local response to the land-use impact has not been fully addressed because there is no available way to reliably separate the local climate change signal from the global one. Only the urban impact has been estimated by comparing observations in cities with those in rural areas. The estimate, however, is limited to urban areas and provides little information about the impact of other land-cover types on the long-term surface temperature trend. In addition, estimates vary with the method of classifying urban and rural areas. For instance, the warming trend due to urbanization over the US estimated by *Easterling et al.*

[1996] based on population is  $+0.06^{\circ}\text{C}/\text{century}$  whereas *Hansen et al.* [2001] based on night-light observation obtain  $+0.15^{\circ}\text{C}/\text{century}$ .

[4] The objective of this study is to assess the surface warming sensitivity to land types and urbanization using the “Observation minus Reanalysis (OMR)” approach [KC; *Zhou et al.*, 2004; *Frauenfeld et al.*, 2005]. Specifically, we apply OMR to estimate the impact of urban areas and other land types for the Northern Hemisphere (NH) based on the comparison between surface temperature trends observed in surface stations with those derived from the NCEP/NCAR reanalysis (NNR) [*Kalnay et al.*, 1996; *Kistler et al.*, 2001] and ECMWF-40 (ERA40) [*Simmons et al.*, 2004]. The rationale for the OMR approach is that while reanalyses represent the large-scale climate changes due to greenhouse gases and atmospheric circulation, the NNR and (to a lesser extent) and the ERA40 are insensitive to regional surface processes associated with different land types [*National Research Council (NRC)*, 2005] because little or no surface data or information about land-surface changes were used in the data assimilation process. Thus, the surface observations after removing the reanalysis enable us to isolate local near-surface warming patterns from the global-scale warming signal. We will attempt to attribute the local OMR surface warming patterns to land types using land type classifications made with satellite observations.

### 2. Data

[5] The NH surface temperature data used in this study consist of two gridded ( $2.5^{\circ} \times 2.5^{\circ}$ ) reanalyses (ERA40 (2-meter temperature from <http://data.ecmwf.int/data/>) and NNR), and two ( $5^{\circ} \times 5^{\circ}$ ) observations (Global Historical Climatology Network (GHCN) [*Peterson and Vose*, 1997], and Climatic Research Unit (CRU) [*Jones and Moberg*, 2003]) from <http://www.ncdc.noaa.gov> and <http://www.cru.uea.ac.uk>, respectively. NCEP/DOE reanalysis version 2 (R2) is also used for investigating OMR time series in section 3. The NNR creates its own estimate of surface fields from the upper air information combined with model parameterizations of surface processes. As a result, the NNR should not be sensitive to local surface properties at all, even if it should show climate change effects to the extent that they affect the observations above the surface [*Kistler et al.*, 2001]. Moreover, it has been shown that a reanalysis made with a frozen model (as the case of the NNR) can detect an anthropogenic trend present in observations assimilated by the reanalysis system essentially at its full strength [*Cai and Kalnay*, 2005]. As to the ERA40, surface temperature and soil moisture are estimated by assimilating the CRU observations in an off-line mode. Therefore, it is expected that the OMR using ERA40 would contain a portion of climate trend due to the impact of land types, resulting in a smaller OMR

<sup>1</sup>Department of Meteorology, Florida State University, Tallahassee, Florida, USA.

<sup>2</sup>Department of Atmospheric and Oceanic Science, University of Maryland at College Park, College Park, Maryland, USA.

<sup>3</sup>School of Earth and Atmospheric Sciences, Georgia Institute of Technology, Atlanta, Georgia, USA.

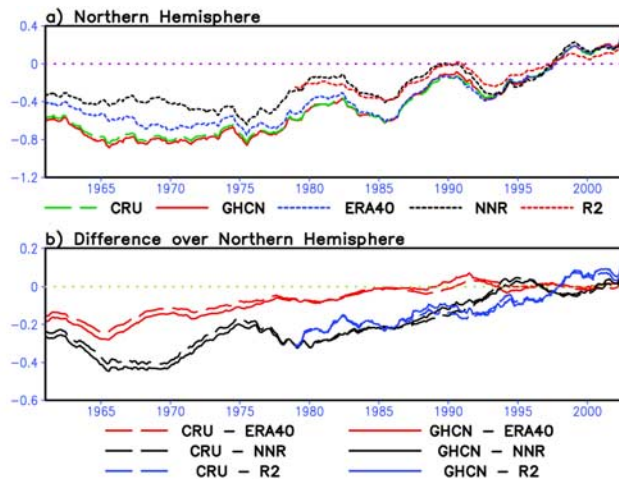


**Figure 1.** Time series (three-year running mean) of (a) land surface temperature anomalies ( $^{\circ}\text{C}$ ) derived from CRU, GHCN, ERA40, NNR, and R2 and (b) the OMRs. Anomaly values are obtained by removing the 30-yr mean from 1961 to 1990 and they are further adjusted to have zero mean over the last 10 years (1993–2002).

trend than that derived from NNR. However, since the surface air temperature observations are used indirectly, it is expected that the OMR applied to ERA40 also has some useful information about land types underneath.

[6] To attribute OMR trend to land types, we used the Moderate Resolution Imaging Spectro-radiometer (MODIS) land cover map [Friedl *et al.*, 2002] from <http://edcdaac.usgs.gov/modis/mod12q1.asp>. The data consist of 16 land types with  $1\text{ km} \times 1\text{ km}$  pixels.

### 3. Hemispheric Surface Temperature Time Series

[7] Plotted in Figure 1 are surface temperature anomalies averaged over the NH derived from three reanalyses and two observations. Anomalies are further adjusted to have zero mean over the last 10 years (1993–2002) because the biases of reanalyses for the most recent years are smallest [Simmons *et al.*, 2004]. The ERA40 time series in Figure 1a is nearly identical to Figure 1 (top) by Simmons *et al.* [2004]. It is seen that the two observations (e.g. CRU and GHCN) are nearly indistinguishable (Figure 1a), showing a gradual warming trend. Reanalyses are in good agreement with the observations in terms of capturing the inter-annual variability and the long-term warming trends. As expected, the upward trend of the ERA40 is closer to observations than both the NNR and its follow-up, R2. Nevertheless, it is evident that the observations exhibit a larger warming trend compared to reanalyses (Figure 1a). As a result, OMRs show a positive trend (Figure 1b), with a larger trend using NNR or R2 than ERA40. This suggests that OMR time series using ERA40, NNR and R2 support the NNR-based findings of KC, namely that the reanalysis trend is smaller than the observations' trend.

### 4. OMR Trends With Respect to Land Types

[8] We now relate OMRs long-term trends to the surface properties. Areal fractions of individual land covers ( $1\text{ km} \times 1\text{ km}$ ) are calculated for each  $5^{\circ} \times 5^{\circ}$  grid, which is the same resolution as the surface temperature data. Displayed

in Figure 2a is the geographic distribution of the dominant land cover types, whose areal percentage in each grid exceeds at least 40% (equivalent to about  $100,000\text{ km}^2$  at  $30^{\circ}\text{N}$ ). In order to avoid ambiguity in classifying dominant types we excluded grid boxes (colored black in Figure 2a) where the dominant type covers less than 40% of the area. A more stringent requirement with higher percentage is not desirable because it would lead to a situation in which the number of the qualified grid points in each category is too small to draw any statistically significant results. Figure 2a includes major land types characterizing the earth surface, as listed in Table 1. However, urban, wetland, closed shrub land, and natural vegetation mosaic are absent in Figure 2a (and no color bar is assigned to these categories) because none of these 4 categories has the largest percentage coverage in any of the  $5^{\circ} \times 5^{\circ}$  grid boxes. We will use the high-resolution MODIS data to assess the urban impact on the long-term surface temperature trend in the next section. Panel (b) displays the mean OMR trends and their vertical error bars at 95% significance level as a function of land type using GHCN/NNR (red) and GHCN/ERA40 (blue), respectively. As in KC, the OMR trend per decade is obtained by taking the average of two decadal mean differences, that is, 90's–80's and 70's–60's, at each grid point, followed by averaging for the same land types. Table 1 lists the number of  $5^{\circ} \times 5^{\circ}$  grid boxes used for the OMR trend calculation for each of the 16 land-cover categories. The OMR calculations were performed only in grid boxes where observation and reanalysis coexist.

[9] The two independent reanalyses appear to reveal a very similar dependence of the OMR trends with respect to land types as well as their statistical significance levels (Figure 2b). This suggests that the attribution of the OMR

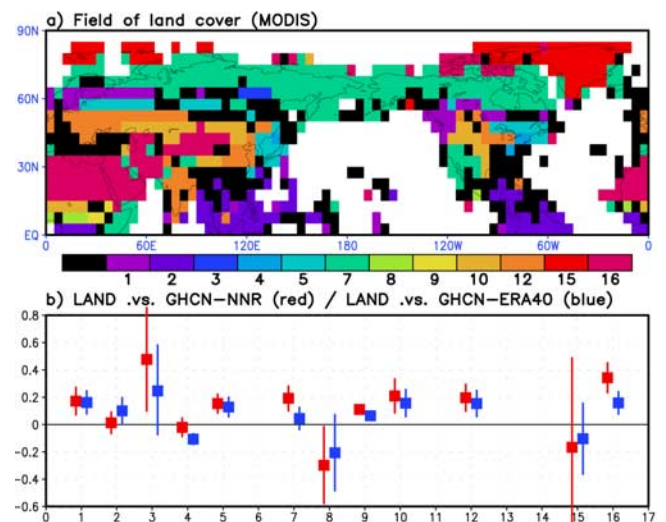


**Figure 2.** (a) Land cover map derived from MODIS. Grid boxes in which the dominant land cover type covers less than 40% are colored black and not used in the analysis presented in Figure 2b. (b) The mean OMR trend of “GHCN-minus-NNR” (red), and “GHCN-minus-ERA40” (blue) per decade ( $^{\circ}\text{C}/\text{decade}$ ) over the NH as a function of land types. Filled squares represent the mean OMR trends and vertical lines the error bars at 95% significance level. The OMR trend per decade is obtained by taking the average of two decadal mean difference (90s-80s and 70s-60s).

**Table 1.** 16 Land-Cover Categories From MODIS and the Number of  $5^\circ \times 5^\circ$  Grid Boxes Used for Calculation of OMR Trends Per Decade

Land Cover Category	Number of Grid Boxes
Evergreen needle-leaf forest	29
Evergreen broadleaf forest	42
Deciduous needle-leaf forest	4
Deciduous broadleaf forest	3
Mixed forest	31
Closed shrubland	0
Open shrubland	81
Woody savannah	6
Savannah	6
Grassland	36
Wetland	0
Cropland	51
Urban	0
Natural vegetation mosaic	0
Snow and ice	3
Barren or sparsely vegetated	56

trends to different land types is robust. The key features in the OMR trends are summarized below:

[10] (i) The OMR trend over barren areas (category 16) ( $\geq 0.3^\circ\text{C}/\text{decade}$ ) is larger than most of the other land types. It is known that the evaporation feedback decreases the surface warming. The results seem to suggest that over barren or arid areas where soil moisture is very limited, the evaporation feedback would be negligible, explaining a larger local surface warming under the same amount of radiative forcings due to anthropogenic greenhouse gases, as discussed by *Dai et al.* [2004] and *Hales et al.* [2004].

[11] (ii) The OMR over croplands and grass (12 and 10), where a large seasonal vegetation change takes place, show a moderate decadal warming ( $\sim 0.2^\circ\text{C}/\text{decade}$ ). In contrast, for the land type 4 (broad-leaf deciduous), which experiences a similarly large seasonal variation in terms of vegetation growth as the cropland, the OMR trend is very small. This suggests human activities could be responsible for an additional local warming.

[12] (iii) In addition, the positive OMR trend is evident over arid areas with shrubs (7) ( $\sim 0.2^\circ\text{C}/\text{decade}$ ). Together with a result in (i), this suggests that the OMR trend could be related to the soil moisture level [*NRC*, 2005].

[13] (iv) There are large OMR trends over the needle-leaf forests (1 and 3) ( $\geq 0.2^\circ\text{C}/\text{decade}$ ), and conversely, broadleaf tree areas (2 and 4) do not show a significant warming trend ( $0.05^\circ\text{C}/\text{decade}$ ). These results are quite consistent with modeling works [*Shukla et al.*, 1990; *Xue and Shukla*, 1993; *Giambelluca et al.*, 1997] which show that reduced (increased) transpiration by clearing (creating) broadleaf forest causes warming (cooling). We therefore suggest that larger transpiration and evaporative cooling over broadleaf forests may be related to weaker warming than needle-leaf forests.

## 5. Urban Impact

[14] Urban impact on surface climate change is also assessed, along with the comparison with impacts of other land types. Grid boxes in which the percentage area of  $1\text{ km} \times 1\text{ km}$  urban pixels exceed 4.3% (between 1 and 4.2%) are categorized as “big” (“small”) urban areas, so that the well-known large cities have been included in the big urban categories (Figure 3a). 4.3%-urban pixels in a

grid box of  $5^\circ \times 5^\circ$  corresponds to an area of approximately  $11,000\text{ km}^2$  at  $30^\circ\text{N}$ . Grid boxes categorized as big urban areas based on this criterion include France, Germany, Italy, and UK in Europe; Beijing, Guangzhou-Hong Kong, Japan, Shanghai, South Korea, and Taiwan in east Asia; California, Chicago, Florida, New York-Boston in North America (Figure 3a). We then examine whether OMR trends over these “extended urban areas” are indeed larger than other areas.

[15] Figure 3 depicts the OMR time series averaged over big urban areas, small urban areas, agriculture, broadleaf forests, and barren areas. The order of magnitude in warming trends, shown in both panels is consistent. Big urban area shows a larger warming trend than small urban and agricultural areas. However, urban warming is weaker than that over barren areas, which are the most sensitive regions in terms of surface warming. OMR decadal warming trends (computed with the same method as in section 4) are 0.24, 0.19, 0.18, 0.03, 0.33 for these five categories using “GHCN-NNR”. The trends using “CRU-NNR” are 0.21, 0.19, 0.2, 0.02, 0.34, respectively. It appears that the barren or urban surface with limited soil moisture exerts a strong surface warming response due to a weaker evaporative cooling process [*Hales et al.*, 2004; *NRC*, 2005]. In contrast, warming trend over natural broadleaf forests is smaller than other land types, supporting the notion that the high soil moisture damps surface warming.

## 6. Summary and Discussion

[16] Prominent features identified from the OMR using reanalyses (NNR or ERA-40) and observational datasets (GHCN or CRU) are:

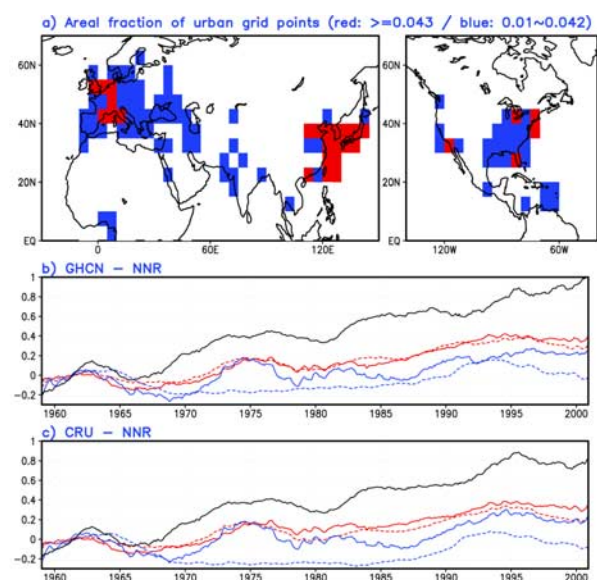


**Figure 3.** (a) Geographical distribution of urban grids ( $5^\circ \times 5^\circ$ ). Grid boxes where the fractional area of  $1\text{ km} \times 1\text{ km}$  urban pixels is greater than 0.043 (in red), and between 0.01 and 0.042 (in blue) are categorized as big (small) urban areas. Time series ( $^\circ\text{C}$ ) of (b) GHCN-NNR, and (c) CRU-NNR, for the areas of big urban areas (red solid), small urban areas (red dashed), agriculture (blue solid), natural broadleaf (blue dashed), and barren areas (black solid), respectively.

[17] 1) Barren areas show a larger warming trend ( $\geq 0.3^\circ\text{C}/\text{decade}$ ) than most of other land types. It should be pointed out that the larger warming over the barren areas may not necessarily be associated with land-cover change, such as desertification or deforestation. For example, large OMR difference over Sahara desert may simply imply that the local surface warming due to greenhouse effects are stronger there because of a much weaker evaporation feedback over the desert [Dai et al., 2004; Hales et al., 2004]. Diffenbaugh [2005] and NRC [2005] discussed that greenhouse gas-induced atmosphere-land cover feedbacks can increase or decrease the local surface temperature by modifying surface albedo, the soil moisture and evaporation process.

[18] 2) Among all other land types, urban impact on surface warming is strongest second to the barren areas. In particular, it exceeds the warming in agricultural land by  $0.06^\circ\text{C}/\text{decade}$ .

[19] 3) Within areas of strong seasonality, agricultural areas (cropland) and mixed forests show a moderate warming trend ( $\sim 0.2^\circ\text{C}/\text{decade}$ ) whereas natural deciduous broad-leaf areas do not. But this may need further reassessment because of the small number of samples for the deciduous broad-leaf class, even if its error bar is very small.

[20] 4) In contrast, for the highly vegetated areas such as tropical forest and low-latitude evergreen broad-leaf tree areas, the strong evaporative cooling appears to suppress the surface warming ( $< 0.1^\circ\text{C}/\text{decade}$ ). Dai et al. [2004] and Kumar et al. [2004] address that surface temperature change is related to the soil moisture, which in turn associated with vegetation types. We suggest that this reasoning is also applicable to explain much larger warming trends in mid-latitude needle-leaf forests than moist broadleaf forests identified in this study.

[21] The results shown here support our hypothesis that the OMR can be attributed to the sensitivity of surface climate change to land types. The findings are mostly insensitive to the choice of reanalyses or observational datasets. It is important to note that this study uses the land cover estimated by recent MODIS observations, which may or may not reflect changes in land types. Therefore, part of the sensitivity of the OMR to land types may be due to changes in land type. There may be also other uncertainties in OMR differences, but the fact that the OMR does provide a statistically significant and physically explainable sensitivity to land type suggests these uncertainties may be random and cancel out after averaging over a large number of grids with same land type. However, it is important to use climate modeling techniques for further understanding of the warming sensitivity to land types and the climate impact of land use changes.

[22] **Acknowledgments.** This study is supported by the National Science Foundation (ATM-0403211 and ATM-0403518) and by the Climate Change Data and Detection program of NOAA Office of Global Programs (GC04-259). ERA40 data were obtained from the ECMWF public web server, <http://data.ecmwf.int/data>. The constructive comments and suggestions from the anonymous reviewer are helpful.

## References

Bounoua, L., et al. (1999), Interactions between vegetation and climate: Radiative and physiological effects of doubled atmospheric  $\text{CO}_2$ , *J. Clim.*, *12*, 309–324.

- Cai, M., and E. Kalnay (2005), Can reanalysis have anthropogenic climate trends without model forcing?, *J. Clim.*, *18*, 1844–1849.
- Dai, A., K. E. Trenberth, and T. Qian (2004), A global dataset of Palmer drought severity index for 1870–2002: Relationship with soil moisture and effects of surface warming, *J. Hydrometeorol.*, *5*, 1117–1130.
- Diffenbaugh, N. S. (2005), Atmosphere-land cover feedbacks alter the response of surface temperature to  $\text{CO}_2$  forcing in the western United States, *Clim. Dyn.*, *24*, 237–251.
- Easterling, D. R., T. C. Peterson, and T. R. Karl (1996), On the development and use of homogenized climate datasets, *J. Clim.*, *9*, 2941–2944.
- Frauenfeld, O. W., T. Zhang, and M. C. Serreze (2005), Climate change and variability using European Center for Medium-Range Weather Forecast analysis (ERA-40) temperatures on the Tibetan Plateau, *J. Geophys. Res.*, *110*, D02101, doi:10.1029/2004JD005230.
- Friedl, M. A., et al. (2002), Global land cover from MODIS: Algorithms and early results, *Remote Sens. Environ.*, *83*, 287–302.
- Gallo, K. P., and T. W. Owen (1999), Satellite-based adjustments for urban heat island temperature bias, *J. Appl. Meteorol.*, *38*, 806–813.
- Giambelluca, T. W., D. Hölscher, T. X. Bastos, R. R. Frazão, M. A. Nullet, and A. D. Ziegler (1997), Observations of albedo and radiation balance over postforest land surfaces in the eastern Amazon basin, *J. Clim.*, *10*, 919–928.
- Hales, K., J. D. Neelin, and N. Zeng (2004), Sensitivity of tropical land climate to leaf area index: Role of surface conductance versus albedo, *J. Clim.*, *17*, 1459–1473.
- Hansen, J. E., R. Ruedy, M. Sato, M. Imhoff, W. Lawrence, D. Easterling, T. Peterson, and T. Karl (2001), A closer look at United States and global surface temperature change, *J. Geophys. Res.*, *106*, 23,947–23,963.
- Intergovernmental Panel on Climate Change (2001), *Climate Change 2001: The Scientific Basis: Contribution of Working Group I to the Third Assessment Report of the Intergovernmental Panel on Climate Change*, edited by J. T. Houghton et al., 881 pp., Cambridge Univ. Press, New York.
- Jones, P. D., and A. Moberg (2003), Hemispheric and large-scale surface air temperature variations: An extensive revision and an update to 2001, *J. Clim.*, *16*, 206–223.
- Kalnay, E., and M. Cai (2003), Impact of urbanization and land-use on climate change, *Nature*, *423*, 528–531.
- Kalnay, E., et al. (1996), The NCEP/NCAR 40-year reanalysis project, *Bull. Am. Meteorol. Soc.*, *77*, 437–471.
- Kalnay, E., et al. (2005), Estimation of the impact of land surface forcings on temperature trends in the eastern United States, *J. Geophys. Res.*, doi:10.1029/2005JD006555, in press.
- Kistler, R., et al. (2001), The NCEP/NCAR 50-year reanalysis: Monthly means CD-ROM and documentation, *Bull. Am. Meteorol. Soc.*, *82*, 247–267.
- Kumar, A., F. Yang, L. Goddard, and S. Schubert (2004), Differing trends in the tropical surface temperatures and precipitation over land and oceans, *J. Clim.*, *17*, 653–664.
- Lofgren, B. M. (1995), Sensitivity of land-ocean circulations, precipitation, and soil moisture to perturbed land surface albedo, *J. Clim.*, *8*, 2521–2542.
- National Research Council (NRC) (2005), *Radiative Forcing of Climate Change: Expanding the Concept and Addressing Uncertainties*, 207 pp., Natl. Acad. Press, Washington, D. C.
- Peterson, T. C., and R. S. Vose (1997), An overview of the Global Historical Climatology Network temperature database, *Bull. Am. Meteorol. Soc.*, *78*, 2837–2848.
- Pielke, R. A., Sr., et al. (2002), The influence of land-use change and landscape dynamics on the climate system: Relevance to climate-change policy beyond the radiative effects of greenhouse gases, *Philos. Trans. R. Soc. London*, *360*, 1–5.
- Shukla, J., C. Nobre, and P. Sellers (1990), Amazon deforestation and climate change, *Science*, *247*, 1322–1325.
- Simmons, A. J., et al. (2004), Comparison of trends and low-frequency variability in CRU, ERA-40, and NCEP/NCAR analyses of surface air temperature, *J. Geophys. Res.*, *109*, D24115, doi:10.1029/2004JD005306.
- Xue, Y., and J. Shukla (1993), The influence of land surface properties on Sahel climate. part I: Desertification, *J. Clim.*, *6*, 2232–2245.
- Zhou, L., R. E. Dickinson, Y. Tian, J. Fang, Q. Li, R. K. Kaufmann, C. J. Tucker, and R. B. Myneni (2004), Evidence for a significant urbanization effect on climate in China, *Proc. Natl. Acad. Sci.*, *101*, 9540–9544.

M. Cai and Y.-K. Lim, Department of Meteorology, Florida State University, Room 418, Love Building, Tallahassee, FL 32306-4520, USA. (cai@met.fsu.edu)

E. Kalnay, Department of Atmospheric and Oceanic Science, University of Maryland at College Park, 3431 Computer and Space Sciences Building, College Park, MD 20742–2425, USA.

L. Zhou, School of Earth and Atmospheric Sciences, Georgia Institute of Technology, 311 Ferst Drive, Atlanta, GA 30332–0340, USA.